DOI: 10.15669/pnst.8.98

Progress in Nuclear Science and Technology
Volume 8 (2025) pp. 98-103

ARTICLE

SIMMER-III Simulation of ULOF Transient in Pu Burner Reactor

Yoshiharu TOBITA*, Xue-Nong CHEN and Andrei RINEISKI

Karlsruhe Institute of Technology, Kaiserstraße 12 76131 Karlsruhe, Germany

In connection with the EU project PuMMA[1,2], a ULOF (Unprotected Loss of Flow) transient of the Pu burner core based on the ESFR-SMART [3-5] design was analyzed[6] with the SIMMER-III code[7,8]. Oscillatory behavior of reactivity and reactor power occurred, caused by the negative reactivity feedback due to coolant boiling above the fissile column, which lowers the reactor power and stops the boiling. In contrast to ESFR-SMART, this oscillation did not lead to prompt criticality in the Pu burner by sodium condensation above the core even with conservative assumptions on reactivity feedback mechanisms. This is due to the increased negative coolant density and/or void reactivity in the sodium plenum due to the reduction in core height in the Pu burner core, thus demonstrating that the Pu burner core has high tolerance to the ULOF transient.

KEYWORDS: SIMMER-III, ULOF, Pu burner, ESFR-SMART reactor, PuMMA Project

I. Introduction

In the context of the PuMMA project,[1,2] which aims to define different options for Pu management in Generation IV nuclear reactors and to evaluate the impact of high plutonium (Pu) content on the whole fuel cycle, reactor safety and performance, the objective of this study was to elucidate the safety characteristics of SFRs used as reactors for the burning of Pu, and to provide insights that could contribute to the future licensing process of SFRs by analyzing a representative severe accident of SFRs, the Unprotected Loss of Flow (ULOF). The target core is based on the ESFR-SMART[3-5] core developed in a European collaborative project. It has been adapted to improve the Pu burning capability. Compared to ESFR-SMART, the target core is of reduced axial dimensions and power, with increased Pu enrichment, while the Pu isotopic composition is assumed to be the same. It can be considered as a "mild" burner compared to the "strong" ones, with similar dimensions and power, but higher Pu enrichment, thinner fuel pins and introduced inert pins, which are currently investigated in the PuMMA scenario studies. We want to proceed step by step in the safety study, therefore we start from the mild burner. The analysis of ULOF in ESFR-SMART[6] using the SIMMER-III code[7,8] showed that neutron leakage and reactor power decrease due to sodium boiling in the sodium plenum during the accident, followed by a subsequent reactor power increase when boiling subsides, indicating oscillatory behavior of reactivity and reactor power. This oscillatory behavior was influenced by feedback effects, such as reactivity feedback due to core thermal expansion, and had been shown to drive core disruption and prompt criticality under certain conditions in ESFR-SMART. The purpose of this study was to elucidate the effect of increased Pu enrichment and reduced core height in the mild Pu burner core on this oscillatory behavior. ULOF event was analyzed with SIMMER-III, and the influence of reactivity feedback mechanisms on the oscillatory behavior was also investigated.

*Corresponding author, E-mail: yoshiharu.tobita@kit.edu

II. Simulation of Pu Burner Core

1. Specification of Pu Burner Core

The radial and axial layout of the Pu burner core is almost similar to ESFR-SMART and is illustrated in **Fig. 1**. The mass balance of Pu and actinides in ESFR-SMART is near zero. To increase the Pu enrichment and realize the Pu and, optionally, minor actinides burning, the height of the core is reduced, and the lower blanket material is replaced with steel pellets of the same diameter as the inner diameter of cladding. The fissile column height is reduced from 75 cm to 50 cm in the inner core, and from 95 cm to 65 cm in the outer core. The Pu fuel enrichment is increased from 18.7% in ESFR-SMART to 22.5% in the inner core and to 21.5% in the outer core. As the core height is reduced to about 2/3, the reactor power is also reduced from 3600 MWth to 2400 MWth and the primary coolant flow is reduced from 18705 kg/s to 12550 kg/s. The reactivity feedback coefficients calculated with SIMMER-III and some related values are shown in **Table 1** and compared with the ESFR-SMART[6] and its reference values.[3] Note that these values are preliminary and may require future reevaluation.

2. SIMMER Code

The SIMMER-IV and SIMMER-III[7] are computational codes that perform a comprehensive analysis of the nuclear thermal-hydraulic behavior of a damaged core. Both codes are capable of simulating a reactor system in three-dimensional Cartesian and two-dimensional cylindrical coordinates, respectively. They are collectively referred to as the SIMMER code, as the physical models in both codes are identical, except for their geometric calculation systems. The

Table 1 Neutronic parameters and feedback coefficients

Parameter	Pu burner SIMMER-III	ESFR-SMART SIMMER-III [6]	Serpent Calculation [2]
Keff	1.00320	1.00937	1.00471
Prompt Neutron Lifetime	4.66E-7 s	4.25E-7 s	4.74E-7 s
Beta effective	350 pcm	347 pcm	362 pcm
Doppler Coeeficient ΔT=300K	-564 pcm	-808 pcm	-685 pcm
Core void worth	1277 pcm	1727 pcm	1542 pcm
Upper gas plenum + Gap void worth	-69.0 pcm	-41.3 pcm	-62 pcm
Sodium plenum void worth	-1275 pcm	-656 pcm	–
Coolant density reactivity (core)	0.331 pcm/K	0.442 pcm/K	0.433 pcm/K
Coolant density reactivity (sodium plenum)	-0.194 pcm/K	-0.136 pcm/K	–
Axial thermal expansion coefficient	-0.119 pcm/K	-0.0715 pcm/K	-0.083 pcm/K
Radial Thermal Expansion Coefficient	-0.980 pcm/K	-0.711 pcm/K	-0.646 pcm/K
Control Rod Drivelines Expansion Coefficient	-423/14.5 pcm/cm	-423/14.5 pcm/cm	-423/14.5 pcm/cm

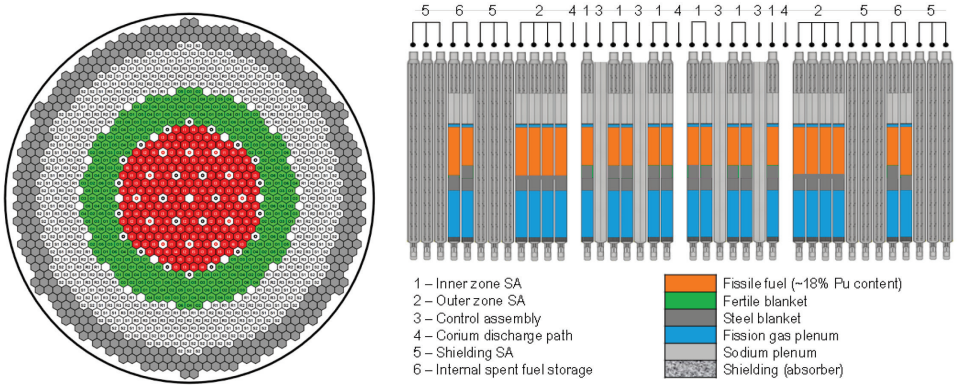

Fig. 1 Radial and axial core map (red: inner core, green: outer core),[5] Fertile blanket is replaced with Steel blanket

SIMMER code is employed to analyze the propagation of the disrupted area within the reactor core and the consequent reactor power changes in the Transition Phase (TP), with a particular focus on the energy generation behavior due to prompt criticality and the conversion of this energy into mechanical energy by core expansion. The code incorporates a fluid dynamics module to calculate the thermal hydraulics of the mixture of degraded core materials, a neutronics module to analyze space-dependent kinetics, and a structure module that considers the melting and failure of structures. SIMMER treats core materials such as fuel, steel, sodium, and FP gas as different components in solid, liquid, and gaseous states. The fluid dynamics module computes multi-velocity field flow, multi-phase, multi-component flow, heat and mass transfer between components, and momentum exchange. Solid particles are treated as fluids, but are treated separately from liquid components. The structure module calculates heat transfer and melting/solidification/failure behavior among fuel elements, sub-assembly walls, and fluid, while fluid convection is limited by the presence of intact sub-assembly walls. The neutronics module calculates reactivity and power from macroscopic cross sections based on mass and temperature distribution of the core material, time-dependent neutron flux being computed using multi-group transport theory and the improved quasi-static scheme.

3. SIMMER Modeling

The cylindrical 2-dimensional SIMMER-III model is set up as shown in **Fig. 2(a)**. The inner core is divided into 8 fuel assembly (FA) rings, while the outer core has 3 FA rings. The secondary loop and the intermediate heat exchanger are modeled in order to simulate the heat exchange with the primary loop and the natural convection circulation in the primary loop after the loss of pump thrust. The pump thrust is given by the inner boundary condition (IBC). The sodium flow in the secondary loop at constant flow rate and inlet temperature is also given by the boundary condition (BC) as shown in **Fig. 2(b)**. In this analysis, the overflow system was not modeled. Therefore, the cover gas pressure increases due to the thermal expansion of sodium in the reactor vessel after the ULOF occurs. For this reason, a constant pressure boundary condition was set in the upper right corner of the reactor vessel. The calculation with constant nominal power and flow rate was performed for 600s to obtain a stabilized steady-state thermal condition as the initial condition for the subsequent ULOF transient

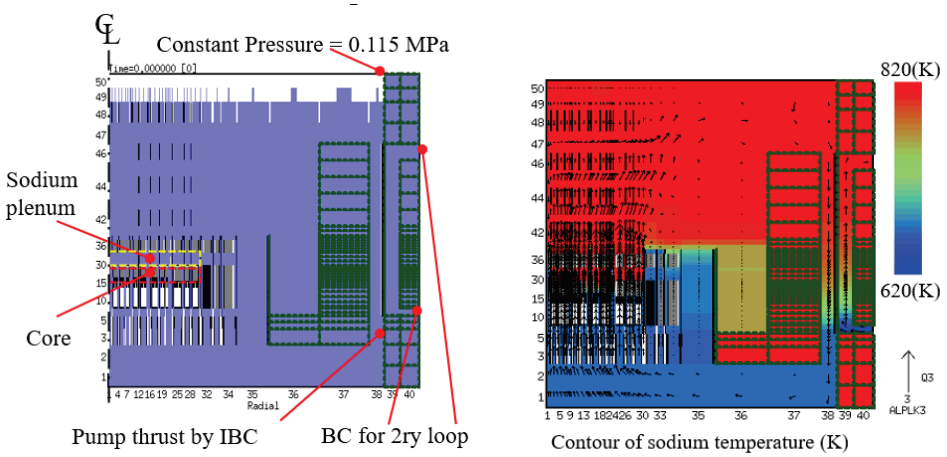

(a) Analytical geometry

(b) Sodium temperature distribution at the rated operation

Fig. 2 Analytical geometry of Pu burner reactor

calculation. The contour of temperature and flow vector of sodium in this steady-state condition are shown in Fig. 2(b). The pump thrust was gradually reduced to zero, simulating a loss of flow with a flow halving time of 10s. **Figure 3** shows the time transient of the flow rate obtained from the analysis. After 40s, the pump thrust becomes 0, and the flow rate due to natural convection is achieved at about 15% of the rated flow rate. The natural convection flow rate shows peaks at about 10s intervals due to sodium boiling in the upper plenum, which will be described later.

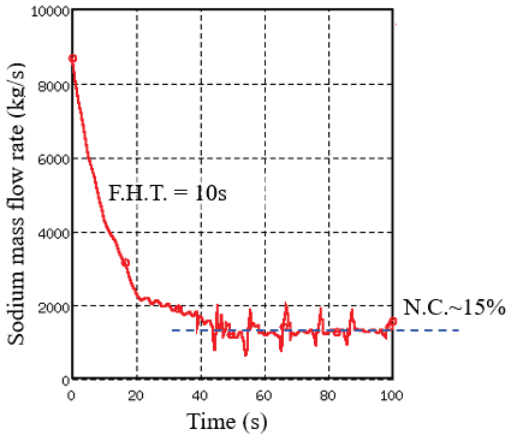

Fig. 3 Transient of sodium mass flow rate

4. Analysis Cases

In this study, several cases were analyzed focusing on the combinations of the reactivity feedback mechanisms by the thermal expansion of the CRDL (Control Rod Drive Line) and the core fuel[9] as shown in **Table 2**. This table shows the combinations in each case analyzed. Since the thermal expansion of the CRDL always inserts the control rod into the core, it is conservative to ignore this. Therefore, in the base case, Case 0, the negative reactivity feedback due to the CRDL thermal expansion is not considered.

The effect of core expansion is somewhat complicated as

Table 2 Calculation cases and conditions

Case	CRDL thermal expansion	Constraint of fuel by cladding in core thermal expansion
Case 0 (base)	off	-
Case 1	off	No
Case 2	on	-
Case 3	on	No
Case 4	on	Yes

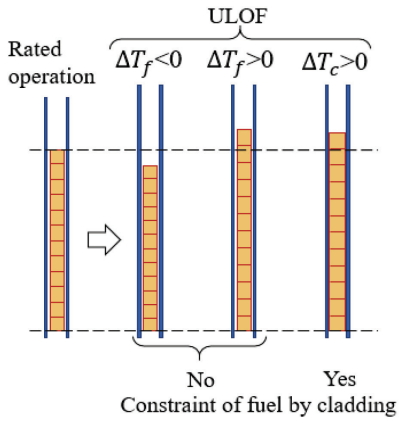

Fig. 4 The thermal axial expansion of core

indicated in **Fig. 4**. If the fuel pellets are not constrained by the cladding, the decrease or increase in fuel temperature will directly result in the contraction or expansion of the core fuel, respectively. On the other hand, if the fuel pellets are constrained by the cladding, the core fuel will expand with the cladding regardless of the fuel temperature change because the cladding temperature change is always positive in ULOF. In Case 0, the reactivity change by the core thermal expansion is not considered, because at the beginning of this study, we didn't have an enough information about the fuel temperature transient in ULOF. As described later, the analysis of Case 0 showed that the

fuel temperature would eventually drop below the rated operating condition. Therefore, in Case 1, an analysis was performed assuming that the fuel pellets were not constrained by the cladding to account for the contraction and reactivity increase due to the drop in fuel temperature. In Cases 2 to 4, the negative reactivity insertion due to thermal expansion of the CRDL was realistically considered. Under this condition, three analysis cases were performed: a case in which the thermal expansion of the core was not considered (Case 2), and a case in which the thermal expansion of the core was considered with (Case 3) and without (Case 4) the restraint of the fuel pellets by the cladding.

III. Results and Discussion

Figure 5 shows the transients of reactivity, reactor power and core averaged fuel temperature in Case 0. The reactor power and reactivity decrease in the first 30s due to the negative reactivity feedback by the temperature increase in sodium plenum and doppler feedback by the fuel temperature increase. After about 25s, the effect of the decrease in reactor power exceeds the effect of the decrease in heat removal due to LOF, and the fuel temperature begins to decrease.

After about 30s, the reactivity and the reactor power begin to oscillate. This oscillation is initiated by the boiling in the sodium plenum, as shown in **Fig. 6**, which shows the reactivity and reactor power transients up to the initial 60s and the material distribution around the core at 45.3s, 50.0s and 55.6s. The blue area in the lower three figures represents liquid sodium volume fraction and the white area sodium vapor. At 45.3s, the boiling in the sodium plenum increases neutron leakage, rapidly reducing reactivity and reactor power. The sodium boiling subsides by this power decrease reducing the neutron leakage and increasing the reactivity

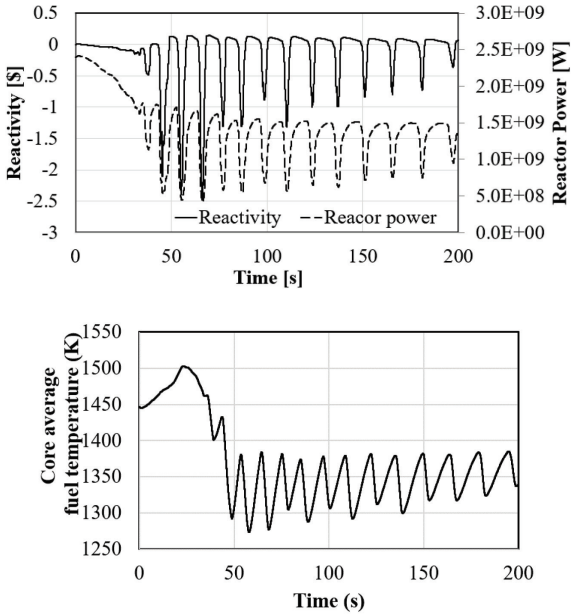

Fig. 5 Transients of the reactivity, the reactor power and the core averaged fuel temperature in Case 0

and reactor power again at 50.0s, leading to an oscillatory behavior of reactivity and reactor power in the same manner thereafter. However, the reactivity peak throughout the oscillation is less than about 0.2$, and the possibility of fuel disruption and prompt criticality driven by this oscillation is thought to be quite small.

As shown in Fig. 5, after about 40s, the fuel temperature becomes lower than the rated operation and the positive reactivity will be inserted due to thermal contraction of the fission column height. The effect of this positive reactivity feedback was simulated using a thermal core expansion model[9] in Case 1. The transient of reactivity and reactor

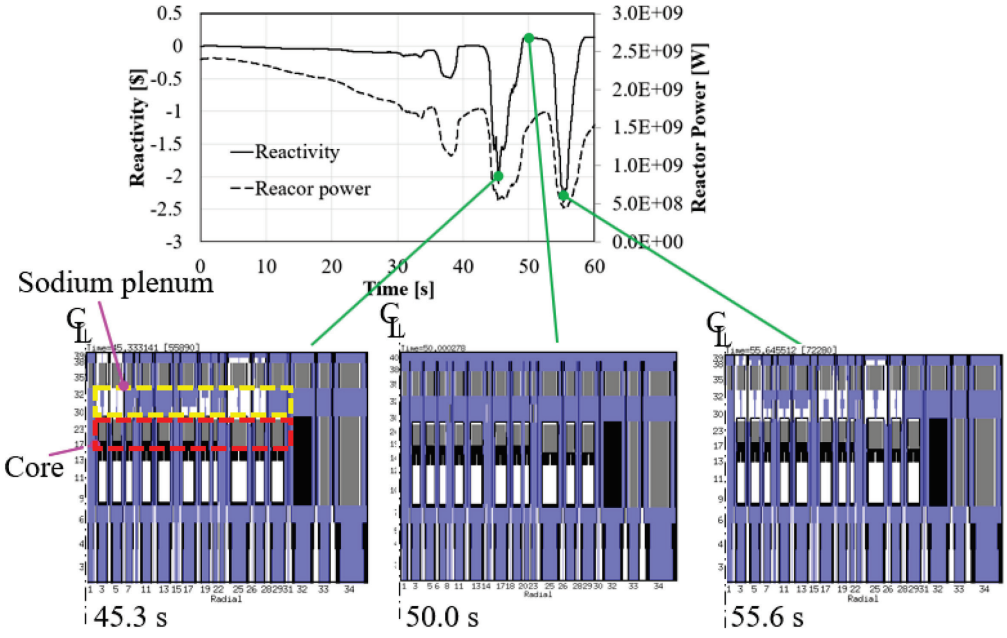

Fig. 6 Reactivity and reactor power transients and material distribution around the reactor core in Case 0

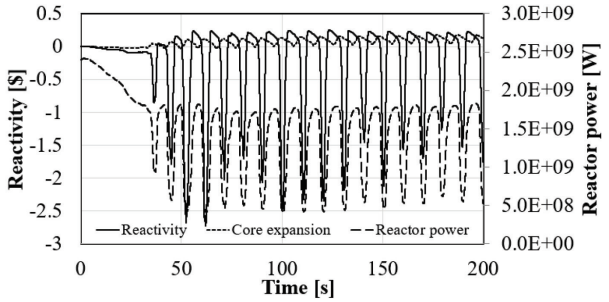

Fig. 7 Transients of the reactivity and the reactor power in Case 1

power is given in **Fig. 7**. The maximum positive reactivity due to core contraction, plotted by the dotted line, is about 0.14$. Moreover, the time of this peak does not coincide with the peak of the reactivity oscillation caused by the repeated onset and subsidence of the sodium plenum boiling. This is because the core contraction is caused by the reduction in reactor power due to the sodium plenum boiling. After all, the reactivity peak during the oscillatory behavior in this case is less than about 0.25$ and prompt criticality will not occur even with the consideration of the positive reactivity feedback by the core contraction. This is in contrast to ESFR-SMART, where the oscillation-driven prompt criticality occurred even though the negative reactivity feedback from thermal expansion of the CRDL was considered together.[6] This difference is due to the increased negative coolant density and/or void reactivity in the sodium plenum as a result of the reduction of the core height in Pu burner core as shown in Table 1.

As shown in Fig. 6, the peak reactivity during oscillation occurs at the moment when the sodium plenum stops boiling and is filled with single-phase coolant, so it is governed by the coolant density reactivity and the coolant temperature. **Figure 8** shows a conceptual diagram of the axial profile of the coolant temperature around the reactor core during rated operation and after ULOF onset. From this figure, one can deduce that the increase in the core average coolant temperature due to ULOF is about half of the temperature increase in the sodium plenum. The coolant density reactivity of the core and sodium plenum in the Pu burner and ESFR-SMART is excerpted from Table 1 and shown again in **Table 3**. In ESFR-SMART, the coolant density reactivity of the core is larger than twice that of the absolute value of sodium plenum, and the coolant temperature rise in

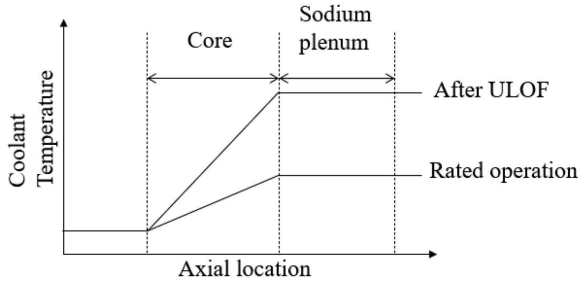

Fig. 8 Conceptual diagram of the axial coolant temperature profile around the core at rated operation and after ULOF onset

Table 3 Coolant density reactivity of the core and sodium plenum in the Pu burner and ESFR-SMART

Parameter	Pu burner	ESFR-SMART
Coolant density reactivity (core)	0.331 pcm/K	0.442 pcm/K
Coolant density reactivity (sodium plenum)	-0.194 pcm/K	-0.136 pcm/K

ULOF will cause a positive reactivity feedback to the reactivity peak in the oscillation. On the other hand, in the case of Pu burner, the coolant density reactivity of the core is less than twice that of the absolute value of sodium plenum, therefore the temperature rise during ULOF results in a negative reactivity feedback. This is thought to be the reason for the difference in the transient behavior between Pu burner and ESFR-SMART. As discussed here, for a design measure to place a sodium plenum just above the reactor core to mitigate the consequences of ULOF, it is important

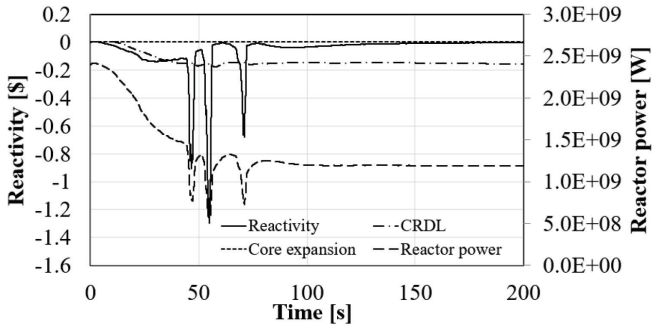

(a) Case 2

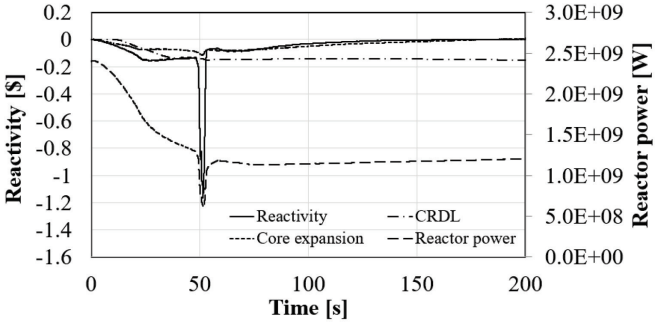

(b) Case 3

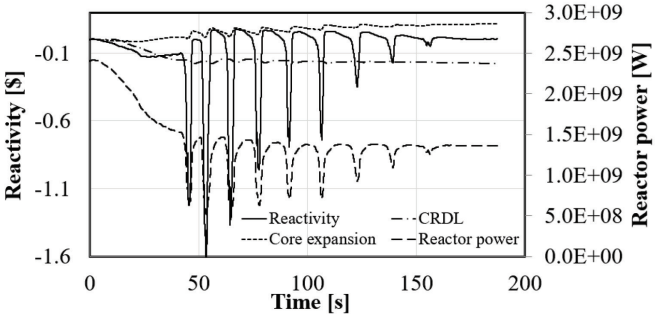

(c) Case 4

Fig. 9 Transients of the reactivity and reactor power in Cases 2 to 4

that the absolute value of the coolant density reactivity of the sodium plenum be less than half that of the reactor core.

Figure 9 shows the results of the cases 2 to 4. These cases realistically considered the negative reactivity feedback due to the thermal expansion of the CRDL. The negative reactivity introduced by the thermal expansion of the CRDL reduced the reactor power more rapidly than in Case 0 and Case 1. Thus, the oscillation due to sodium boiling subsided after a few times. This also holds true in Case 4, where the positive reactivity insertion due to fuel contraction is considered.

IV. Conclusion

The ULOF transient of the mild Pu burner reactor, which was designed by modifying the design of the ESFR-SMART reactor, was analyzed using the SIMMER-III code. Similar to the ESFR-SMART reactor, oscillations in reactivity and reactor power were observed due to the onset and cessation of sodium boiling in the sodium plenum adjacent to the top of the fissile column. Even with the positive reactivity feedback from core thermal shrinkage and without negative reactivity feedback from CRDL thermal expansion, the prompt criticality is judged not to occur in the Pu burner core because the peak reactivity during the oscillation is less than about 0.25$. This is due to the increased negative coolant density and/or void reactivity in the sodium plenum due to the reduction in core height in the Pu burner core, thus demonstrating that the Pu burner core has high tolerance to the ULOF transient. The reactivity feedbacks in strong burners considered in the PuMMA scenario studies may differ due to different Pu isotopic compositions and higher Pu enrichments in fuel pins, safety studies for these strong burners are planned for PuMMA and subsequent projects.

Acknowledgment

This study contributes to the European PuMMA project, Plutonium Management for More Agility, receiving funding from the EU Horizon 2020 program, grant agreement 945022. The content of this paper reflects only the authors' views and the European Commission cannot be held responsible for them. The authors would like to express their gratitude to the JAEA for the provision of SIMMER under a JAEA-KIT/CEA agreement on the exchange of information and collaboration to develop the code.

References

1) N. Chauvin, F. Álvarez-Velarde, et al., "PuMMA, a European project devoted to Plutonium Management for More Agility," 3M-01-04, *Proc. Int. Nucl. Fuel Cycle Conf. (GLOBAL2024)*, October 6-10, Tokyo, Japan.
2) PuMMA Project, https://pumma-h2020.eu/ , 2024
3) K. Mitiyuk, J. Krepei, E. Girardi, "ESFR-SMART: new Horizon-2020 project on SFR safety," IAEA-CN245-450, *Proc. Int. Conf. on Fast Reactors and Related Fuel Cycles (FR17)*, Yekaterinburg, Russia, 26-29 June (2017).
4) A. Rineiski, C. Meriot, et al., "ESFR-SMART Core Safety Measures and Their Preliminary Assessment," *J. Nucl. Eng. and Rad. Sci*., **8**, January (2022).
5) E. Fridman, K. Mikityuk, ESFR-SMART T1.2.1 Vademecum. Technical report (2019).
6) X.-N. Chen, A. Rineiski, et al., *Annals of Nuclear Energy*, **183** (2023) 109642.
7) Y. Tobita, et al., "The Development of SIMMER-III, An Advanced Computer Program for LMFR Safety Analysis and Its Application to Sodium Experiments," *Nuclear Technology*, **153**[3], 245-255 (2006).
8) S. Kondo, Y. Tobita, et al., "SIMMER-III and SIMMER-IV: Computer Codes for LMFR Core Disruptive Accident Analysis," *JAEA-Research 2024-008*, October (2024).
9) L. Andriolo, A. Rineiski, et al., "An Innovative Methodology for Evaluating Core Thermal Expansion Feedbacks in Transient Analyses," Paper 15292, *Proc. ICAPP 2015*, pp. 504-512, Paper 15292, May 03-06, Nice, France (2015).